Atmos. Chem. Phys., 23, 1565–1578, 2023
https://doi.org/10.5194/acp-23-1565-2023

Atmospheric Chemistry and Physics
Open Access
EGU

Fates of secondary organic aerosols in the atmosphere identified from compound-specific dual-carbon isotope analysis of oxalic acid

Buqing Xu[1,2], Jiao Tang[1,2], Tiangang Tang[1,3], Shizhen Zhao[1,2], Guangcai Zhong[1,2], Sanyuan Zhu[1,2], Jun Li[1,2], and Gan Zhang[1,2]

[1]State Key Laboratory of Organic Geochemistry, Guangzhou Institute of Geochemistry, Chinese Academy of Sciences, Guangzhou 510640, China
[2]CAS Center for Excellence in Deep Earth Science, Guangzhou 510640, China
[3]Key Laboratory of Agro-ecological Processes in Subtropical Region, Institute of Subtropical Agriculture, Chinese Academy of Sciences, Changsha, 410125, China

Correspondence: Gan Zhang (zhanggan@gig.ac.cn)

Received: 6 October 2022 – Discussion started: 1 November 2022
Revised: 10 January 2023 – Accepted: 11 January 2023 – Published: 27 January 2023

Abstract. Secondary organic aerosols (SOAs) are important components of fine particulates in the atmosphere. However, the sources of SOA precursor and atmospheric processes affecting SOAs are poorly understood. This limits our abilities to improve air quality and model aerosol-mediated climate forcing. Here, we use novel compound-specific dual-carbon isotope fingerprints ($\Delta^{14}C$ and $\delta^{13}C$) for individual SOA tracer molecules (i.e., oxalic acid) to investigate the fates of SOAs in the atmosphere at five emission hotspots in China. Coal combustion and vehicle exhaust accounted for ∼ 55 % of the sources of carbon in oxalic acid in Beijing and Shanghai, but biomass burning and biogenic emissions accounted for ∼ 70 % of the sources of carbon in oxalic acid in Chengdu, Guangzhou, and Wuhan during the sampling period. The dual-carbon isotope signatures of oxalic acid and bulk organic carbon pools (e.g., water-soluble organic carbon) were compared to investigate the fates of SOAs in the atmosphere. Photochemical aging and aqueous-phase chemical processes dominate the formation of oxalic acid in summer and in winter, respectively. The results indicated that SOA carbon sources and chemical processes producing SOAs vary spatially and seasonally, and these variations need to be included in Chinese climate projection models and air quality management practices.

1 Introduction

Great efforts have been made to decrease fine-particle ($PM_{2.5}$) pollution in China, which led to a great improvement in air quality during the last decade. However, $PM_{2.5}$ concentrations in Chinese urban areas are still much higher than the World Health Organization guideline (Xing et al., 2020). Further improvements in air quality will be difficult to achieve because primary particulate emissions have already been effectively controlled through stringent regulatory polices established since 2005 (Zhao et al., 2018), and emissions of volatile organic compounds have remained stable (Wang et al., 2021). Field observations have indicated that most organic aerosols in Chinese urban areas are secondary organic aerosols (SOAs) formed through oxidation of biogenic and anthropogenic precursor volatile organic compounds in the atmosphere (Huang et al., 2014). Our poor understanding of SOAs leads to some of the most important uncertainties when assessing global/regional climate forcing, either directly through solar radiation scattering and absorption or indirectly through aerosol–cloud interactions (Carlton et al., 2009; Hallquist et al., 2009). The sources of SOAs and chemical processes affecting SOAs in polluted areas of China need to be better understood to allow air quality control strategies to be optimized and accurate simulations of climate forcing to be developed.

The large variety of SOA precursors and the complexity of physical/chemical processes in the real atmosphere render great challenges in understanding SOA formation. Radiocarbon ($\Delta^{14}C$) measurements of organic aerosol components allow high-precision fingerprinting to be achieved and the relative contributions of fossil fuels and biogenic/biomass sources to be determined (Gustafsson et al., 2009; Zhang et al., 2021). The $\Delta^{14}C$ values for bulk organic aerosol materials such as black carbon (BC), organic carbon (OC), and water-soluble organic carbon (WSOC) have been determined (Andersson et al., 2015; Szidat et al., 2004, 2006; Kirillova et al., 2013; Liu et al., 2014), but it is still difficult to directly measure the $\Delta^{14}C$ values of SOAs in atmospheric aerosols, which are chemically complex. Molecular-level $\Delta^{14}C$ analysis of SOA markers can overcome this problem and remove uncertainty caused by using bottom-up organic precursor emission inventories (Chang et al., 2022).

Oxalic acid is a useful SOA marker because it is a key end product of various transformation pathways in the atmosphere and is typically the most abundant SOA component (Boreddy and Kawamura, 2018; Kawamura and Bikkina, 2016; Myriokefalitakis et al., 2011). Stable-carbon-isotope measurements ($\delta^{13}C$) of oxalic acid have been widely used to differentiate between various atmospheric processes affecting organic aerosols (Aggarwal and Kawamura, 2008; Wang et al., 2020; Zhang et al., 2016; Shen et al., 2022; Qi et al., 2022). Estimated kinetic isotope effects indicate that secondary formation and photochemical aging will affect $\delta^{13}C$ in opposite ways (Kirillova et al., 2013). Combining $\delta^{13}C$ and $\Delta^{14}C$ measurements of oxalic acid could therefore allow the carbon sources of SOAs to be identified and processes affecting SOAs in the ambient atmosphere to be investigated.

In this study, we determined the dual-carbon isotope fingerprints ($\Delta^{14}C$ and $\delta^{13}C$) of water-soluble SOA components (oxalic acid and related polar organic acids) and their parent water-soluble aerosols (i.e., WSOC) in five highly industrialized and populated megacities in China. The cities were Beijing, Chengdu, Guangzhou, Shanghai, and Wuhan, which were used to represent the five main regional carbon emission hotspots in China (the North China Plain, the Sichuan Basin, the Pearl River Delta, the Yangtze River Delta, and the middle reaches of the Yangtze River, respectively) (Fig. S1 in the Supplement). We determined spatial and seasonal variations in the sources of carbon in oxalic acid in the study areas. We then compared the $\delta^{13}C$ and $\Delta^{14}C$ data for oxalic acid and the bulk organic aerosol pool to investigate the atmospheric processes affecting SOAs in the different cities and seasons. The molecular-level isotope fingerprints allowed observational constraints on the sources of carbon in SOAs and atmospheric processes affecting SOAs to be determined. The results improve our understanding of the fates of SOAs in the atmosphere.

2 Methods

2.1 Sampling campaign

Field sampling was performed in five megacities: Beijing, Chengdu, Guangzhou, Shanghai, and Wuhan. The locations of the cities are shown in Fig. S1. Sampling was performed at an urban site and a suburban site in each city so that city-level data were acquired. The sampling campaign was described previously (Zhao et al., 2021), and sampling information is shown in Table S1. At each site, $PM_{2.5}$ samples were collected onto pre-combusted Whatman quartz-fiber filters (20 cm × 25 cm) using a high-volume sampler and a flow rate of 1 m^3 min^{-1}. Two intensive sampling campaigns were performed at each sampling site, with consecutive 24 h samples collected for 1 week in January 2018 (winter) and July 2018 (summer). A single sample representing the winter or summer at a sampling site was prepared by combining 1/10 of a portion of each filter collected in a sampling campaign at the site. A total of 20 pooled samples were prepared and used in the subsequent experiments. One field blank sample for each site was collected and analyzed. The samples were stored at −20 °C until they were analyzed.

2.2 Extracting water-soluble ions, WSOC, and dicarboxylic acids

Each pooled sample was extracted four times. Each extraction involved adding 50 mL of ultrapure water to the sample and ultrasonicating the sample for 30 min. The extracts were combined and passed through a 0.22 µm polytetrafluoroethylene membrane filter. Each extract was divided into several portions of different volumes, and the different portions were analyzed to determine the concentrations and/or carbon isotope compositions of water-soluble ions, WSOC, and dicarboxylic acids.

The carbon content of the WSOC was determined using a total organic carbon analyzer (TOC-VCPH, Shimadzu, Kyoto, Japan) following the non-purgeable organic carbon analysis method (Kirillova et al., 2010). Water-soluble inorganic ions (Ca^{2+}, Cl^-, K^+, Mg^{2+}, Na^+, NH_4^+, NO_3^-, and SO_4^{2-}) were determined using a Metrohm 761 Compact IC ion chromatograph (Metrohm, Herisau, Switzerland). The WSOC and water-soluble inorganic ion concentrations in duplicate samples were determined, and the concentrations were corrected for the concentrations in the field blanks (Mo et al., 2021).

2.3 Dicarboxylic acid analysis and carbon isotope analysis

The stable-carbon-isotope $\delta^{13}C$ and radiocarbon $\Delta^{14}C$ values for dicarboxylic acids were determined using previously published methods (Xu et al., 2021). Briefly, an ultrapure water extract of a sample was evaporated to dryness and then derivatized with 10 % BF_3 in 1-butanol (Sigma-Aldrich,

St Louis, MO, USA) at 100 °C for 1 h to convert carboxyl groups into butyl ester groups. The derivatives were extracted with *n*-hexane and quantified by gas chromatography–mass spectrometry before isotope analysis was performed. The $\delta^{13}C$ values for individual diacids were determined by gas chromatography–isotope ratio mass spectrometry (Thermo Fisher Scientific Delta V, Waltham, MA, USA). Each sample was analyzed in triplicate, and the analytical errors for the replicate analyses were generally < 0.3 ‰.

Compound-specific radiocarbon analysis of oxalic acid was achieved by separating and harvesting single compounds using a preparative capillary gas chromatograph in sufficient quantities to allow offline natural-abundance ^{14}C measurements to be made by accelerator mass spectrometry. The preparative capillary gas chromatography isolates were rinsed with dichloromethane, completely dried, and combusted at 920 °C with CuO and Ag in a quartz tube to give CO_2. The CO_2 was purified in a vacuum system and then reduced to graphite using the hydrogen reduction method. The $\Delta^{14}C$ value was determined using the 1.5 SDH-1, 0.5 MV compact accelerator mass spectrometry facility (NEC, National Electrostatics Corporation, USA) at the Guangzhou Institute of Geochemistry of the Chinese Academy of Sciences (Zhu et al., 2015). Each accelerator mass spectrometry analysis ^{14}C result is reported as a fraction modern (F_m) normalized to a common $\delta^{13}C$ value of -25 ‰. The results were corrected for background carbon using an isotope dilution method described in previous publications (Xu et al., 2021). The $\delta^{13}C$ and F_m values for individual diacids were calculated using the relevant isotope ratios for diacid derivatives and 1-butanol using an isotope mass balance equation. Each F_m result was converted into a "fraction of contemporary carbon" (F_c) by normalizing the F_m using a conversion factor of 1.06 to correct for excess ^{14}C from nuclear bomb tests (Xu et al., 2022).

2.4 Carbon isotope analysis of WSOC

A $\sim$ 15 mL aliquot of a WSOC extract was cooled to -20 °C and dried in a vacuum freeze drier. The residue was redissolved in $\sim$ 200 µL of ultrapure water, then 50 µL was transferred to a tin capsule for stable-carbon-isotope analysis, and 150 µL was transferred to a capsule for radiocarbon analysis. The samples in the capsules were evaporated to dryness at 60 °C before isotope analyses were performed.

The carbon isotopes in the WSOC were determined using a previously published procedure (Mo et al., 2021). The $\delta^{13}C$ value for WSOC was determined using a Flash 2000 elemental analyzer connected to a Delta V ion ratio mass spectrometer (Thermo Fisher Scientific, Waltham, MA, USA). The $\Delta^{14}C$ values for the WSOC samples were determined at the accelerator mass spectrometry facility (1.5 SDH-1, 0.5 MV, NEC, USA). Generally, > 200 µg of WSOC was combusted and converted into graphite for each radiocarbon analysis.

3 Results and discussion

3.1 Spatiotemporal variations in dicarboxylic acids

Dicarboxylic acid, oxocarboxylic acid, and α-dicarbonyl concentrations in the $PM_{2.5}$ samples collected in the winter and summer in the five megacities were determined, and a total of 29 water-soluble organic species were identified, as shown in Table S2. The diacid and related compound concentrations were slightly higher at the urban than suburban sites, but the differences were not significant. For each city, the mean of the concentrations found at the urban and suburban sites is therefore presented.

The total diacid concentrations in the samples from the five megacities were 25–1300 ng m^{-3} (mean $\pm$ standard deviation: 690 ± 360 ng m^{-3}), which were similar to concentrations previously found in other Asian megacities such as Chennai (mean of 610 ng m^{-3}) (Pavuluri et al., 2010) and Hong Kong (mean of 690 ng m^{-3}) (Ho et al., 2006) and slightly lower than concentrations found in 14 Chinese cities in 2003 (890 ± 460 ng m^{-3}) (Ho et al., 2007). Oxalic acid was the most abundant diacid at all of the sampling sites and contributed 70 %–89 % (mean of 82 %) of the total diacid concentrations. The mean ratios of oxalic acid to total diacid concentration were significantly higher than the mean of 58 % found for 14 urban sites in China in 2003 (Ho et al., 2007). The increase in the ratio of oxalic acid to total diacid concentration between 2003 and 2018 indicated that secondary organic aerosol production in China increased between 2003 and 2018 because oxalic acid is an end product of the oxidation of many precursors (Ervens et al., 2011; Carlton et al., 2007; Lim et al., 2010, 2013). Malonic acid and succinic acid were approximately equally the second-most abundant diacids, contributing 4.4 % and 4.7 %, respectively, of the total diacid concentrations, and phthalic acid, terephthalic acid, adipic acid, and azelaic acid were the next most abundant diacids. The mean oxoacid concentration was 54 ± 34 ng m^{-3}, and glyoxylic acid and pyruvic acid were the most and second-most abundant oxoacids, respectively. Two α-dicarbonyls (important oxalic acid precursors) were also determined (Fu et al., 2008; Warneck, 2003). Methylglyoxal was more abundant than glyoxal, and this was partly attributed to the rate of oxidation by OH radicals being lower for methylglyoxal than glyoxal (Meng et al., 2018).

In Beijing (in North China), the diacid concentration was markedly lower in winter (260 ng m^{-3}) than summer (850 ng m^{-3}) (Fig. 1), probably because weaker solar radiation and lower temperatures caused less photochemical oxidation to occur in winter than summer (Ho et al., 2007). In particular, during the winter sampling period, clean air masses originating in Siberia dominated the atmosphere in Beijing (Fig. S2) and may have caused the secondary aerosol precursor concentrations to be very low. In contrast, the ratios of winter to summer diacid concentration for the cities in South China (Chengdu, Guangzhou, Shanghai, and Wuhan)

were > 1 (range of 1.4–4.2) (Fig. 1). Unlike for Beijing, strong photochemical oxidation would have occurred in winter in the cities in South China (Ho et al., 2007). The diacid concentrations were probably higher in winter than summer because the mixing heights were lower, and precipitation was less frequent in winter than summer. Oxocarboxylic acids and α-dicarbonyls had similar spatial and seasonal patterns to diacids, the concentrations being higher in South China in winter than summer but higher in North China in summer than winter.

3.2 Radiocarbon-based oxalic acid source apportionment

We determined the $\Delta^{14}C$ values for oxalic acid (the most abundant diacid) in the samples. The sources of oxalic acid were apportioned based on the $\Delta^{14}C$ data, and the non-fossil contributions to the oxalic acid concentrations (f_{NF}-oxalic acid) were 40 %–76 % (mean of 61 % ± 11 %), as shown in Table S3. The high proportion of f_{NF}-oxalic acid demonstrates that even in the heavily populated and industrialized areas of China, non-fossil emissions are important and ubiquitous sources of oxalic acid. The important non-fossil sources of oxalic acid may be seasonally produced biogenic precursors and precursors emitted during biomass burning. The f_{NF}-oxalic acid values were higher for the suburban sites than the urban areas except for Shanghai (Table S3). This is consistent with larger quantities of fossil fuels being consumed in urban areas than suburban areas. However, intraurban differences were not marked, so the $\Delta^{14}C$-based source apportionment results for the different cities were compared.

The mean f_{NF}-oxalic acid value was higher in summer (67 % ± 10 %) than winter (54 % ± 11 %), indicating that more emissions were caused by fossil fuel combustion, and/or fewer biogenic emissions occurred in winter than summer. In winter, fossil-fuel-derived carbon contributed ∼ 60 % of the carbon in oxalic acid in Beijing and Shanghai (Fig. 2) but < 40 % of the carbon in oxalic acid in Chengdu, Guangzhou, and Wuhan. This agreed with the results of a previous study in which the sources of SOA during winter haze events were apportioned using two complementary bilinear receptor models, and fossil sources were found to contribute 63 %, 50 %, and 35 % of SOAs in Beijing, Shanghai, and Guangzhou, respectively (Huang et al., 2014). Oxalic acid was therefore a good surrogate for SOA.

In summer, a mean of 71 % ± 4 % of the oxalic acid in Chengdu, Guangzhou, Shanghai, and Wuhan (in South China) was derived from natural biomass (Fig. 2). However, a large proportion (56 %) of the oxalic acid in Beijing (in North China) was derived from fossil carbon (Fig. 2). Biogenic precursors are expected to be more important in summer than winter, but fossil-fuel-derived carbon contributed most of the oxalic acid in Beijing in both summer and winter. Back trajectories indicated that the air masses in Beijing during the summer sampling periods mostly originated over the Beijing–North China Plain (Fig. S2), which is one of the most polluted parts of China (Andersson et al., 2015; Zhao et al., 2021).

The concentrations of oxalic acid derived from non-fossil sources and fossil fuel were 190–660 ng m^{-3} (mean of 370 ± 150 ng m^{-3}) and 81–520 ng m^{-3} (mean of 260 ± 150 ng m^{-3}), respectively (Fig. 2). In winter, the concentrations of oxalic acid derived from fossil fuel were higher in cities in South China than in Beijing. The concentrations of oxalic acid derived from fossil fuel were markedly lower in summer than winter in the cities in South China but higher in summer than winter in Beijing. In summer, the concentrations of oxalic acid derived from fossil fuel were 3–5 times higher in Beijing than in the cities in South China (Fig. 2). This would have been caused by seasonally dependent fossil fuel consumption and meteorological conditions, as discussed above.

Oxalic acid derived from non-fossil sources made substantial contributions to or even dominated the oxalic acid in the cities we studied (Fig. 2). The concentrations of non-fossil oxalic acid in the cities in South China were higher in winter than summer. However, biogenic compounds (e.g., isoprene (Bikkina et al., 2014, 2021) and monoterpene (Link et al., 2021)) may contribute a smaller proportion of non-fossil oxalic acid in winter than summer. The high non-fossil oxalic acid concentrations found in winter may therefore have been caused by local and regional biomass burning. As shown in Fig. 3a, the non-fossil oxalic acid concentrations positively correlated with the concentration of non-sea-salt potassium (nss-K^+; a marker for biomass burning) ($r^2 = 0.81$, $p < 0.001$), indicating that the high non-fossil oxalic acid concentrations were mainly caused by emissions of precursors through biomass burning. The slope of the regression line fitted to a plot of the non-fossil oxalic acid concentration against the nss-K^+ concentration (0.49 ± 0.06; Fig. 3a) was similar to the slope found in a previous study performed in the Pearl River Delta area in South China (0.55 ± 0.08) (Xu et al., 2022). When the biomass burning contribution was very low (nss-$K^+ = 0$ µg m^{-3}), the mean non-fossil oxalic acid concentration (190 ng m^{-3}; Fig. 3a) was half of the mean total oxalic acid concentration (370 ng m^{-3}). This suggested that biogenic emissions and biomass burning contributed equally to the mean total oxalic acid concentration.

Non-fossil oxalic acid and nss-K^+ were less abundant in all of the cities in summer than in winter (Fig. 3a), indicating that most of the non-fossil oxalic acid was produced through biogenic emissions in summer. On average, the non-fossil oxalic acid concentrations in Guangzhou, Wuhan, and Chengdu were 1.3, 2.5, and 3.2 times higher, respectively, in winter than summer (Fig. 3a), mostly because more biomass burning occurs in winter than summer. Less marked seasonal variations in non-fossil oxalic acid concentrations were found for Beijing and Shanghai (Fig. 3a), indicating that biomass burning may produce only a small proportion of the oxalic acid found in these cities. This is consistent with emis-

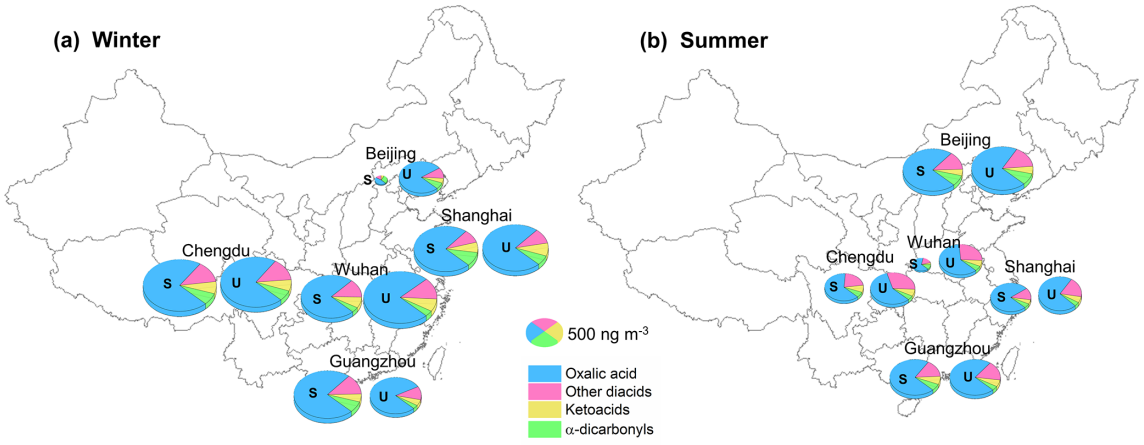

Figure 1. Dicarboxylic acid, oxocarboxylic acid, and α-dicarbonyl concentrations in $PM_{2.5}$ collected in five Chinese megacities in **(a)** winter and **(b)** summer. Samples were collected at a suburban site (S) and an urban site (U) in each city.

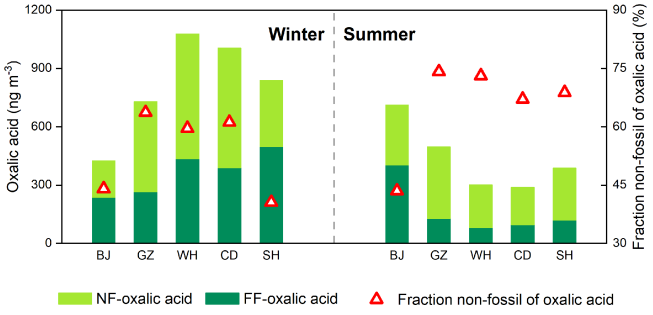

Figure 2. Mass concentrations of oxalic acid derived from non-fossil sources (NF) and fossil fuel (FF) and the mean proportions of non-fossil oxalic acid found for Beijing (BJ), Guangzhou (GZ), Wuhan (WH), Chengdu (CD), and Shanghai (SH) in winter and summer.

sion control legislation being stricter in Beijing and Shanghai than the other cities, meaning biomass burning activities (e.g., crop residue burning) are effectively controlled in Beijing and Shanghai (Qiu et al., 2016). The oxalic acid sources apportioned using the $\Delta^{14}C$ data suggested that decreasing the concentrations of precursors derived from fossil fuels could be important for controlling SOA production in Beijing and Shanghai. In contrast, decreasing the concentrations of precursors derived from both fossil fuels and biomass combustion will be required to decrease the SOA concentrations in areas such as Chengdu, Guangzhou, and Wuhan.

3.3 Relationships between stable-carbon-isotope shifts and atmospheric processing

The stable-carbon-isotope composition ($\delta^{13}C$) provides useful information about the sources of carbon and particularly about atmospheric processes affecting organic compounds. Primary emissions from various sources have different $\delta^{13}C$ values. The $\delta^{13}C$ value will change because of kinetic iso-

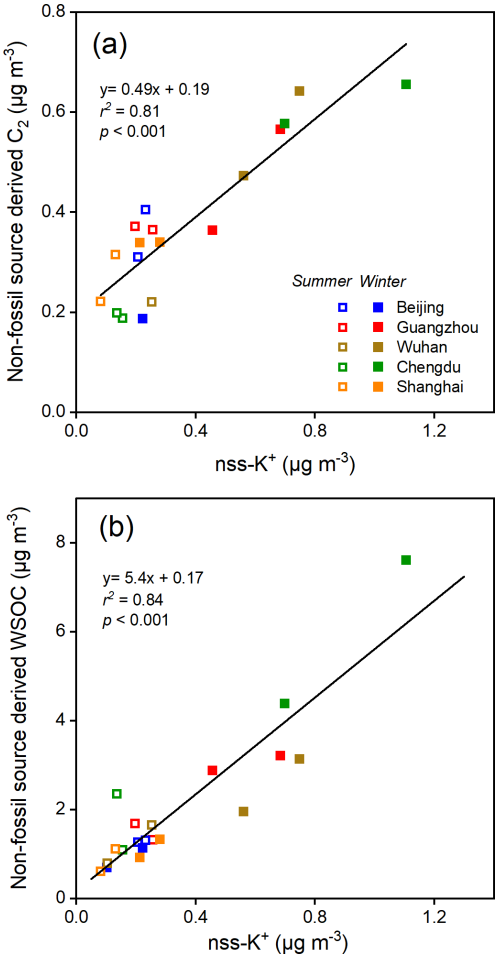

Figure 3. Relationships between **(a)** non-fossil-derived oxalic acid concentrations and non-sea-salt potassium (nss-K^+) concentrations and between **(b)** non-fossil-derived, water-soluble organic carbon (WSOC) concentrations and nss-K^+ concentrations.

tope effects during atmospheric processes (Kirillova et al., 2013) such as oxidation, secondary formation, oligomerization, and gas–particle partitioning (Bikkina et al., 2017b) in which lighter and heavier isotopes behave differently, although source mixing can also affect the $\delta^{13}C$ value. The $\delta^{13}C$ values of diacids therefore have been used widely to track atmospheric processes and assess the degree of organic aerosol aging (Aggarwal and Kawamura, 2008; Zhang et al., 2016; Wang et al., 2020; Shen et al., 2022; Qi et al., 2022).

The $\delta^{13}C$ values for the main diacids and oxoacids in the five cities that were studied are shown in Fig. 4 and Table S4. Oxalic acid had a markedly lower $\delta^{13}C$ (by 4.4 ‰) in winter than summer (Fig. 4). This would have been caused by differences in isotope fractionation caused by atmospheric processes in winter and summer, differences in oxalic acid sources in winter and summer, or a combination. The $\delta^{13}C$ values for the diacids with more carbon atoms (C_3–C_9 diacids) in winter and summer were not very (< 1.5 ‰) different (Fig. 4), so differences in emission sources were not likely to be responsible for the marked seasonal differences in oxalic acid $\delta^{13}C$ values. The nss-SO_4^{2-}-to-SO_4^{2-} ratio ($97\% \pm 3\%$) and nss-K^+-to-K^+ ratio ($94\% \pm 4\%$) indicated that marine emissions with heavier $\delta^{13}C$ signatures did not make marked contributions (Dasari et al., 2019) (Fig. S3), particularly in the coastal cities Guangzhou and Shanghai. The seasonal differences in the $\delta^{13}C$ values could have been stronger for oxalic acid than diacids with more carbon atoms because processes involving isotope fractionation affected diacids with fewer carbon atoms more than diacids with more carbon atoms. The short-chain glyoxylic acid is an important precursor of oxalic acid (Bikkina et al., 2017a; Carlton et al., 2007; Lim et al., 2013) that also had markedly different $\delta^{13}C$ values (by 4.7 ‰) in winter and summer (Fig. 4). The clear seasonal differences in the $\delta^{13}C$ values for oxalic acid and glyoxylic acid suggested that atmospheric processes markedly affected oxalic acid and glyoxylic acid, which are small molecules.

Oxalic acid can be emitted from primary sources, but most oxalic acid in atmospheric aerosol is formed through aqueous-phase reactions and/or photochemical aging, i.e., secondary sources (Huang and Yu, 2007; Van Pinxteren et al., 2014; Xu et al., 2022). During aqueous-phase reactions, the reactivity of isotopically lighter carbon (^{12}C) is higher compared to that of isotopically heavier carbon (^{13}C), and this will cause the $\delta^{13}C$ values to be lower for the particulate products than the gaseous reactants (Anderson et al., 2004; Fisseha et al., 2009; Irei et al., 2006). In contrast, photochemical aging processes can give gaseous products (e.g., CO_2, CO, and volatile organic compounds) which will be enriched in lighter isotopes, causing $\delta^{13}C$ to be higher for the residual (aged) aerosols than the gaseous oxidation products (Aggarwal and Kawamura, 2008; Pavuluri and Kawamura, 2012).

It has been found in several previous studies that aqueous-phase processes play important roles in SOA formation in China in winter (Gkatzelis et al., 2021; Lv et al., 2022; Yu et al., 2021; Wang et al., 2021). This was largely caused by the growth of aerosol liquid water content (ALWC) because the hygroscopic particles were abundant in winter (Yu et al., 2021; Wang et al., 2020; Chen et al., 2021). Ammonium, nitrate, and sulfate are the most important hygroscopic particles in areas with intense anthropogenic emissions (Wu et al., 2018; Lv et al., 2022). As shown in Table S5, the nitrate concentrations were 9 times higher in winter than summer, and the ammonium concentrations were 2.5 times higher in winter than summer. The inorganic aerosol (Ca^{2+}, Cl^-, K^+, Mg^{2+}, Na^+, NH_4^+, NO_3^-, and SO_4^{2-}) contents and meteorological parameters (temperature and relative humidity) were used in the ISORROPIA-II thermodynamic model (Xu et al., 2022), and the results indicated that the ALWCs in all five cities were markedly higher in winter ($60 \pm 76\ \mu g\ m^{-3}$) than summer ($8.5 \pm 5.1\ \mu g\ m^{-3}$) (Table S5). The increase in ALWC in winter may facilitate the partitioning of water-soluble organic precursors to the aqueous phase of the aerosol and promote the subsequent formation of low-volatility compounds such as oxalic acid in the aqueous phase. Meanwhile, aerosols will be less aged in winter than summer because the temperature is lower, and less solar radiation is present in winter than summer. Assuming that source mixing made a minor contribution, the atmospheric processes aging and aqueous SOA formation would have strongly contributed to seasonal variations in the $\delta^{13}C$ values for oxalic acid in the five Chinese megacities that were studied.

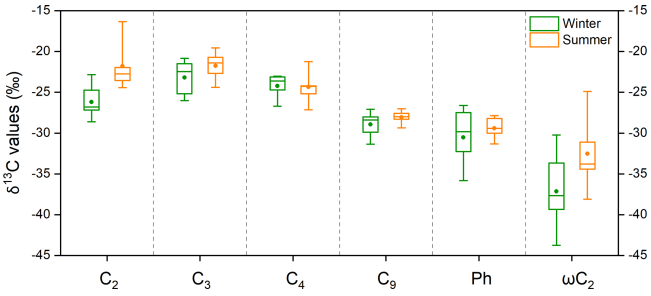

Figure 4. Box-and-whisker plot of the $\delta^{13}C$ values for four saturated aliphatic dicarboxylic acids (C_2, C_3, C_4, and C_9), phthalic acid (Ph), and glyoxylic acid (ωC_2) in $PM_{2.5}$ collected in five Chinese megacities in January 2018 (winter) and July 2018 (summer). Each box indicates the median (the line within the box), the mean (the solid dot within the box), the interquartile range (the ends of the box), and the 10th and 90th percentiles (the whiskers).

3.4 Tracing sources and aerosol processing using the $\delta^{13}C$ and $\Delta^{14}C$ values

Aerosol sources and atmospheric processes affecting aerosols were investigated using the $\delta^{13}C$ and $\Delta^{14}C$ values for oxalic acid, as shown in Fig. 5a. As shown in Fig. 5a, the $\delta^{13}C$ value was higher, and the $\Delta^{14}C$ value indicated more

biogenic oxalic acid was present in summer than winter. The oxalic acid data for Chengdu, Guangzhou, and Wuhan strongly overlap in the plot, suggesting that oxalic acid in these cities had similar sources and had been subjected to similar processes. In contrast, the $\delta^{13}C$ and $\Delta^{14}C$ values for oxalic acid in Beijing and Shanghai are spread over a large area in the plot, indicating that oxalic acid in these cities had various sources and had been subjected to various atmospheric processes. The fossil-carbon contributions to oxalic acid were markedly higher in Beijing and Shanghai than the other cities, as described above. However, the $\delta^{13}C$ values were lower in Beijing and higher in Shanghai. The $\delta^{13}C$ values suggested that organic aerosols in Beijing were predominantly fresh SOAs but that organic aerosols were more affected by photochemical aging in Shanghai than the other cities.

The mean dual-carbon isotope signals for the WSOC pool in the five cities were determined and are shown as gray triangles in Fig. 5a for comparison with the signals for oxalic acid. The aging process is more important in summer than winter, but the mean $\delta^{13}C$ values for WSOC in summer ($-24.8‰ \pm 0.9‰$) and winter ($-24.1‰ \pm 0.4‰$) were not markedly different (Fig. S4). The $\Delta^{14}C$ data for WSOC indicated that the mean non-fossil-carbon contribution to WSOC was $62\% \pm 10\%$ (range of 45 %–80 %; Fig. S4), which was similar to the contribution in 10 Chinese cities in 2013 (mean of $60\% \pm 9\%$, range of 38 %–81 %) (Mo et al., 2021). The WSOC concentration was almost 2 times higher in winter than summer, but the non-fossil-carbon contributions to WSOC in winter and summer were similar ($61\% \pm 11\%$ in winter versus $60\% \pm 9\%$ in summer; Fig. 5a). As shown in Fig. 3b, the non-fossil WSOC concentration significantly correlated with the biomass burning marker (nss-K^+) concentration ($r^2 = 0.84$, $p < 0.001$). When the biomass burning contribution was very low (nss-$K^+ \approx 0\,\mu g\,m^{-3}$), the non-fossil WSOC concentration was close to $0\,\mu g\,m^{-3}$ (Fig. 3b). Unlike oxalic acid, for which biogenic emissions and biomass burning were equally important sources, most of the non-fossil WSOC was associated with biomass burning. The similar WSOC source patterns in winter and summer were therefore probably caused by fossil fuel combustion and biomass burning emissions having similar seasonal variations.

As mentioned above, the average $\delta^{13}C$ and $\Delta^{14}C$ values for WSOC remain almost stable between winter and summer (Fig. 5a), mainly because the source patterns of WSOC were similar in different seasons. Bulk aerosol pools such as WSOC consist of both the reactants and products of the photochemical reactions. Therefore, the isotopic fractionation effects during atmospheric processes would introduce only minor changes in the $\delta^{13}C$ values of WSOC. Oxalic acid contributed a mean of 5.5 % (range of 1.4 %–10.7 %) of the WSOC concentration and was probably the most abundant compound (Myriokefalitakis et al., 2011). However, the carbon isotope compositions of oxalic acid were significantly

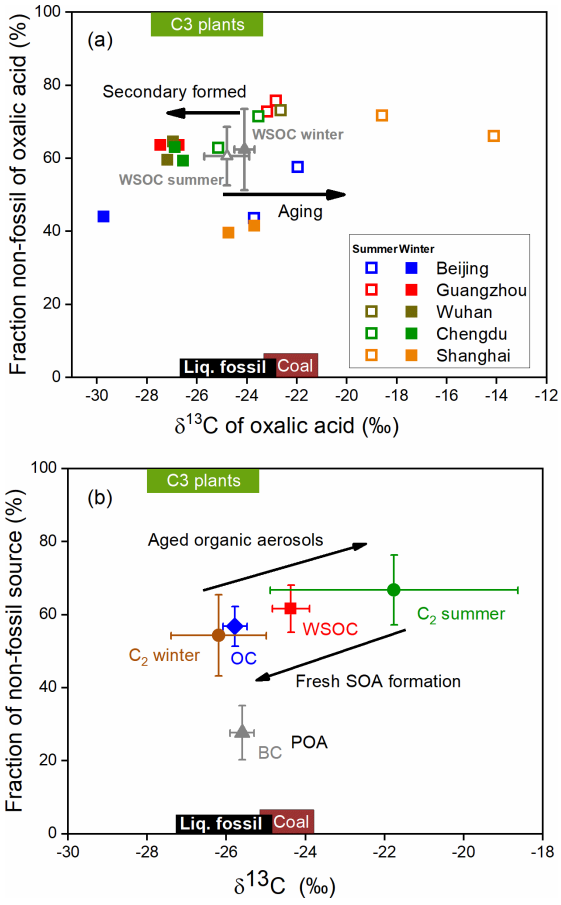

Figure 5. ^{14}C-based non-fossil source fractions plotted against the $\delta^{13}C$ values for molecules and carbonaceous aerosol components. **(a)** Aerosol oxalic acid collected in Beijing (blue), Guangzhou (red), Wuhan (brown), Chengdu (green), and Shanghai (orange) in summer (open squares) and winter (filled squares). The mean dual-carbon isotope signals for water-soluble organic carbon (WSOC) in the five cities in summer (open gray triangles) and winter (filled gray triangles) are also shown (Fig. S4). Each error bar indicates the standard deviation. **(b)** Annual-mean values for black carbon (BC, gray triangles), organic carbon (OC, blue diamonds), WSOC (red squares), and oxalic acid (C_2, brown and green circles) in the five cities (see Table 1 for detailed data and references). Each error bar indicates the standard deviation. Here POA and SOA refer to primary organic aerosol and secondary organic aerosol, respectively. The expected dual-carbon signatures for coal, liquid fossil carbon, and C_3 plants were taken from previous publications (Widory et al., 2004; Huang et al., 2006; Kawashima and Haneishi, 2012; Smith and Epstein, 1971; Martinelli et al., 2002; Cao et al., 2011).

different between winter and summer (Fig. 6). This suggested that oxalic acid could have different carbon sources and be affected by different atmospheric processes between winter and summer.

The $\delta^{13}C$ values of oxalic acid were higher, and the $\Delta^{14}C$ values indicated more oxalic acid than WSOC was formed from non-fossil carbon in summer (Figs. 5a and 6a). The

$\delta^{13}C$ value has been found to increase as the number of carbon atoms in diacids decreases (Aggarwal and Kawamura, 2008; Pavuluri et al., 2011), suggesting that shorter-chain diacids, which can form through photochemical aging of longer-chain diacids, will become enriched in ^{13}C during aging. The $\delta^{13}C$ values of the WSOC pool would refer to both the reactants and products of the atmospheric processes. Enrichment of ^{13}C in oxalic acid relative to WSOC (Fig. 6a) therefore probably reflected that oxalic acid was a photochemical aging product (remaining reactant) in WSOC aerosols in summer. The $\Delta^{14}C$ values indicated more oxalic acid than WSOC was formed from non-fossil carbon in summer (Fig. 6a). This could have been because fossil-carbon components are more recalcitrant than biomass and biogenic components of organic aerosols to oxidative aging (Elmquist et al., 2006; Kirillova et al., 2014a, b), meaning aged oxalic acid (with a higher $\delta^{13}C$ value) will preferentially form from non-fossil carbon (with a higher $\Delta^{14}C$ value). As discussed above, biogenic emissions made larger contributions of oxalic acid than WSOC in summer, which gave the same results.

In contrast, the $\delta^{13}C$ values were lower, and the $\Delta^{14}C$ values indicated more oxalic acid than WSOC was formed from fossil carbon in winter (Figs. 5a and 6b). The lower $\delta^{13}C$ values for oxalic acid found in winter suggested that oxalic acid indicates a freshly formed SOA product in WSOC aerosols, opposite to remaining reactants in summer. WSOC aerosols are mixtures of primary organic aerosols (e.g., sugars) and SOAs. Only a small fraction of water-soluble primary organic aerosols would have had fossil fuel sources (Liu et al., 2014; Mo et al., 2021). Therefore, a higher fossil-carbon contribution to water-soluble SOA than WSOC aerosol was expected, and this was indicated by the $\Delta^{14}C$ values for oxalic acid indicating important fossil-carbon sources. It has been suggested that substantial fossil-carbon-derived precursors are probably oxidized to give water-soluble SOAs through aqueous-phase chemical processes, giving products such as oxalic acid with lower $\delta^{13}C$ values and higher fossil-carbon contributions (Xu et al., 2022). Aqueous-phase processes are facilitated by a high ALWC, which is higher in winter than summer because the hygroscopic particle (e.g., ammonia and nitrate) mass is higher in winter than summer (Lv et al., 2022; Xu et al., 2022), and meteorological conditions (e.g., the boundary layer height, temperature, and wind speed) are unfavorable in winter (Gkatzelis et al., 2021). Photochemical aging is suppressed in winter because of lower temperatures and weaker solar radiation than in summer. This means that more aqueous-phase production of fresh SOA than aerosol photochemical aging will occur in urban areas in China in winter.

3.5 Comparison with carbonaceous aerosol components

The $\delta^{13}C$ and $\Delta^{14}C$ values for oxalic acid were compared with the mean annual isotope compositions of the bulk carbonaceous aerosols (i.e., BC, OC, and WSOC) in $PM_{2.5}$ found in the five study areas in previous studies (Fig. 5b and Table 1). Non-fossil-source-derived carbon was the dominant contributor of OC and WSOC aerosols, the mean annual contributions being $57\,\% \pm 5\,\%$ and $62\,\% \pm 6\,\%$, respectively (Fig. 5b). The large contribution of non-fossil carbon to OC and WSOC (a sub-fraction of OC) contrasted strongly with the large contribution of fossil carbon ($72\,\% \pm 7\,\%$) to BC (Fig. 5b). This was probably because OC aerosols are more affected than BC by biogenic emissions and biomass burning.

The $\delta^{13}C$ values were higher, and the $\Delta^{14}C$ values indicated smaller contributions of fossil carbon for WSOC than OC in both winter and summer (Fig. 5b). Similar results have been found at other locations and for different aerosol sizes (Kirillova et al., 2013, 2014a, b; Bosch et al., 2014), and this was explained by atmospheric aging affecting water-soluble organic aerosols more than organic aerosols. SOA formation typically causes $\delta^{13}C$ to decrease, so fresh secondary production of WSOC from fossil carbon would be less likely. However, the sources and processes affecting the different aerosol components were masked in the mean isotope contents of the aerosol mixtures. Oxalic acid is one of the most abundant compounds in WSOC aerosols. The $\delta^{13}C$ values were lower for the oxalic acid than the WSOC, and the $\Delta^{14}C$ values indicated that fossil carbon made larger contributions to the oxalic acid than the WSOC aerosol in winter (Fig. 5b). The marked differences between the different organic aerosol components indicated that dual-carbon-isotope studies of more aerosol molecules and components should be performed to improve our understanding of the origins and evolution of organic aerosols in the atmosphere.

4 Conclusions

The $\Delta^{14}C$ and $\delta^{13}C$ values of oxalic acid in five megacities in China gave valuable information about the sources of carbon in SOAs and atmospheric processes affecting SOAs. The method allowed the fates of SOA in the atmosphere in urban areas to be investigated even though SOAs are very complex. The SOA sources apportioned from the ^{14}C values indicated marked seasonal variations, non-fossil carbon being dominant in summer and fossil carbon and non-fossil carbon making similar contributions in winter. Precursors containing fossil carbon emitted through coal combustion or by vehicles were mostly responsible for SOA formation in Beijing and Shanghai. SOA formation was mainly associated with precursors containing non-fossil carbon emitted through biomass burning and/or biogenic emissions in Chengdu, Guangzhou, and Wuhan.

Table 1. Compilation of literature values of $\delta^{13}C$ compositions and ^{14}C-based non-fossil source fraction (f_{NF}) for black carbon (BC), organic carbon (OC), water-soluble organic carbon (WSOC), and oxalic acid in $PM_{2.5}$ samples collected from Beijing, Shanghai, Guangzhou, Chengdu, and Wuhan.

Components	Location	Season	$\delta^{13}C$ (‰)	f_{NF} (%)	References
BC	Beijing	Annual	NA*	21	Zhang et al. (2015)
	Beijing	Annual	NA	18	Zhang et al. (2017)
	Beijing	Annual	−24.6	24	Fang et al. (2018)
	Beijing	Summer/winter	−25.8	NA	Cao et al. (2011)
	Shanghai	Summer/winter	−25.9	NA	Cao et al. (2011)
	Shanghai	Annual	−25.6	30	Fang et al. (2018)
	Guangzhou	Summer/winter	−25.9	NA	Cao et al. (2011)
	Guangzhou	Annual	−25.3	25	Fang et al. (2018)
	Chengdu	Annual	−26.1	41	Fang et al. (2018)
	Wuhan	Summer/winter	−25.4	NA	Cao et al. (2011)
	Wuhan	Winter	NA	26	Liu et al. (2016b)
	Average		-25.6 ± 0.3	28 ± 7	
OC	Beijing	Summer/winter	−26.0	NA	Cao et al. (2011)
	Beijing	Annual	NA	52	Zhang et al. (2017)
	Beijing	Annual	NA	50	Liu et al. (2020)
	Shanghai	Summer/winter	−25.8	NA	Cao et al. (2011)
	Shanghai	Winter	NA	51	Huang et al. (2014)
	Shanghai	Annual	NA	53	Liu et al. (2020)
	Guangzhou	Summer/winter	−26	NA	Cao et al. (2011)
	Guangzhou	Annual	NA	55	Liu et al. (2020)
	Guangzhou	Spring	NA	54	Liu et al. (2016a)
	Chengdu	Autumn	NA	73	Liu et al. (2017)
	Wuhan	Summer/winter	−25.6	NA	Cao et al. (2011)
	Wuhan	Winter	NA	62	Liu et al. (2016b)
	Wuhan	Autumn	NA	66	Liu et al. (2017)
	Average		-25.9 ± 0.3	57 ± 5	
WSOC	Beijing	Summer/winter	−24.4	55	This work
	Shanghai	Summer/winter	−23.6	53	This work
	Guangzhou	Summer/winter	−24.8	63	This work
	Chengdu	Summer/winter	−24.7	72	This work
	Wuhan	Summer/winter	−23.6	65	This work
	Beijing	Annual	−23.7	56	Mo et al. (2021)
	Shanghai	Annual	−24	58	Mo et al. (2021)
	Guangzhou	Annual	−24.7	59	Mo et al. (2021)
	Chengdu	Annual	−24.9	69	Mo et al. (2021)
	Wuhan	Annual	−24.3	67	Mo et al. (2021)
	Average		-24.4 ± 0.5	62 ± 6	
Oxalic acid	Beijing	Summer	−22.8	50.5	This work
	Shanghai	Summer	−16.3	68.8	This work
	Guangzhou	Summer	−23	74.2	This work
	Chengdu	Summer	−24.3	67.1	This work
	Wuhan	Summer	−22.4	73.1	This work
	Beijing	Winter	−25.8	44.1	This work
	Shanghai	Winter	−24.2	40.6	This work
	Guangzhou	Winter	−27.1	63.7	This work
	Chengdu	Winter	−26.7	61.2	This work
	Wuhan	Winter	−27.1	62.1	This work
	Average	Summer	-21.8 ± 3.1	67 ± 10	
	Average	Winter	-26.2 ± 1.2	54 ± 11	

* NA – not available.

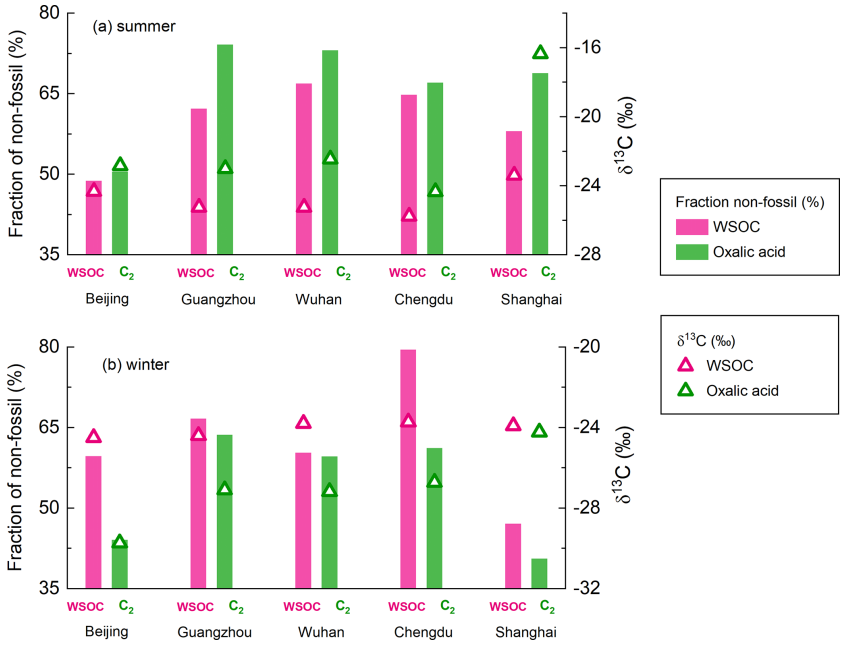

Figure 6. Proportions of non-fossil sources (determined from the ^{14}C values) and δ^{13}C values for water-soluble organic carbon (WSOC) and oxalic acid (C_2) in Beijing, Guangzhou, Wuhan, Chengdu, and Shanghai in **(a)** summer and **(b)** winter.

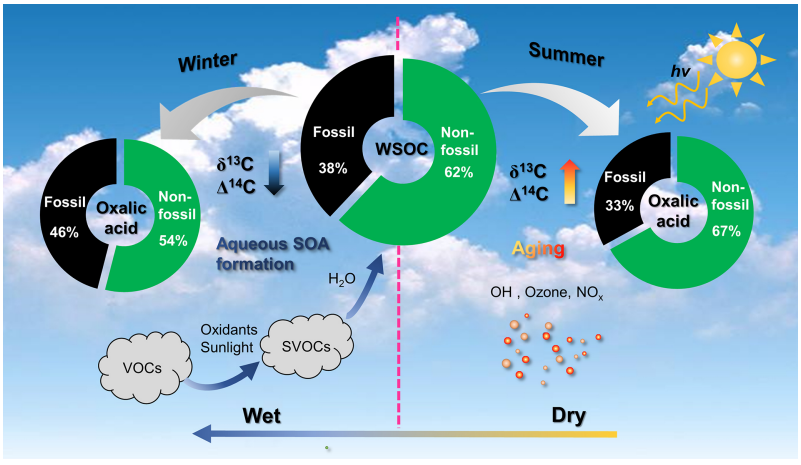

Figure 7. Schematic of the atmospheric fates of secondary organic aerosols (SOAs) in winter and summer. VOCs: volatile organic compounds; SVOCs: semi-volatile organic compounds; WSOC: water-soluble organic carbon.

The dual-carbon-isotope datasets for the individual SOA molecules and bulk organic aerosols indicated that there were two opposite seasonal organic aerosol evolution processes. The fates of SOAs in the atmosphere in winter and summer are shown in Fig. 7. In winter, the high hygroscopic particle mass and unfavorable meteorological conditions (low temperature and high humidity) increase aerosol liquid water formation, which causes fossil-derived, water-soluble gaseous organic precursors to dissolve in the aerosol liquid water and aqueous SOA to form (Fig. 7). Oxalic acid indicates freshly formed aqueous SOA in winter because the δ^{13}C values were lower for oxalic acid than WSOC, and the contribution of fossil carbon was higher for oxalic acid than WSOC. In summer, organic aerosols are more affected by photochemical aging than fresh SOA formation because of the high temperature and the high amount of solar radiation present (Fig. 7). Oxalic acid was affected by SOA aging in summer, and the δ^{13}C and Δ^{14}C values were higher for oxalic acid than WSOC.

In this study, one pooled sample was used to represent the winter or summer at a sampling site. Future compound-specific dual-carbon isotope studies covering a wide range of the temporal and spatial scale are strongly warranted to gain deeper insight into the fates of SOAs in China. Overall, we

found that the carbon sources and SOA evolution processes were markedly different in different cities and seasons. There is a need to include the large spatial and seasonal variations in SOA fates (including precursor sources, SOA formation through gas-phase oxidation and from aqueous-phase chemicals, and SOA aging) in climate projection models and air quality management in China.

Data availability. The data underlying the findings of this study are available in this article (Figs. 1–7 and Table 1) and its Supplement. The derived data generated in this research will be shared on reasonable request to the corresponding author (Gan Zhang).

Supplement. The supplement related to this article is available online at: https://doi.org/10.5194/acp-23-1565-2023-supplement.

Author contributions. GaZ and BX designed the study. GuZ and ShZ provided the samples. BX, JT, and SaZ carried out the measurements. BX processed data and wrote the paper. GaZ, TT, and JL commented on the manuscript.

Competing interests. The contact author has declared that none of the authors has any competing interests.

Disclaimer. Publisher's note: Copernicus Publications remains neutral with regard to jurisdictional claims in published maps and institutional affiliations.

Acknowledgements. We thank Gareth Thomas from Liwen Bianji (Edanz) (https://www.liwenbianji.cn, last access: 23 September 2022) for editing the language of a draft of this paper.

Financial support. This work was funded by the Natural Science Foundation of China (grant nos. 42030715 and 42192511); the Alliance of International Science Organizations (grant no. ANSO-CR-KP-2021-05); the Natural Science Foundation of Guangdong Province, China (grant nos. 2017BT01Z134 and 2022A1515011679); and the China Postdoctoral Science Foundation (grant no. 2022M720143).

Review statement. This paper was edited by Katye Altieri and reviewed by two anonymous referees.

References

Aggarwal, S. G. and Kawamura, K.: Molecular distributions and stable carbon isotopic compositions of dicarboxylic acids and related compounds in aerosols from Sapporo, Japan: Implications for photochemical aging during long-range atmospheric transport, J. Geophys. Res.-Atmos., 113, D14301, https://doi.org/10.1029/2007jd009365, 2008.

Anderson, R. S., Huang, L., Iannone, R., Thompson, A. E., and Rudolph, J.: Carbon Kinetic Isotope Effects in the Gas Phase Reactions of Light Alkanes and Ethene with the OH Radical at 296 ± 4 K, J. Phys. Chem. A, 108, 11537–11544, https://doi.org/10.1021/jp0472008, 2004.

Andersson, A., Deng, J., Du, K., Zheng, M., Yan, C., Skold, M., and Gustafsson, O.: Regionally-varying combustion sources of the January 2013 severe haze events over eastern China, Environ. Sci. Technol., 49, 2038–2043, https://doi.org/10.1021/es503855e, 2015.

Bikkina, S., Kawamura, K., Miyazaki, Y., and Fu, P.: High abundances of oxalic, azelaic, and glyoxylic acids and methylglyoxal in the open ocean with high biological activity: Implication for secondary OA formation from isoprene, Geophys. Res. Lett., 41, 3649–3657, https://doi.org/10.1002/2014gl059913, 2014.

Bikkina, S., Kawamura, K., and Sarin, M.: Secondary organic aerosol formation over coastal ocean: inferences from atmospheric water-soluble low molecular weight organic compounds, Environ. Sci. Technol., 51, 4347–4357, https://doi.org/10.1021/acs.est.6b05986, 2017a.

Bikkina, S., Andersson, A., Ram, K., Sarin, M. M., Sheesley, R. J., Kirillova, E. N., Rengarajan, R., Sudheer, A. K., and Gustafsson, Ö.: Carbon isotope-constrained seasonality of carbonaceous aerosol sources from an urban location (Kanpur) in the Indo-Gangetic Plain, J. Geophys. Res.-Atmos., 122, 4903–4923, https://doi.org/10.1002/2016jd025634, 2017b.

Bikkina, S., Kawamura, K., Sakamoto, Y., and Hirokawa, J.: Low molecular weight dicarboxylic acids, oxocarboxylic acids and α-dicarbonyls as ozonolysis products of isoprene: Implication for the gaseous-phase formation of secondary organic aerosols, Sci. Total Environ., 769, 144472, https://doi.org/10.1016/j.scitotenv.2020.144472, 2021.

Boreddy, S. K. R. and Kawamura, K.: Investigation on the hygroscopicity of oxalic acid and atmospherically relevant oxalate salts under sub- and supersaturated conditions, Environ. Sci.-Proc. Imp., 20, 1069–1080, https://doi.org/10.1039/c8em00053k, 2018.

Bosch, C., Andersson, A., Kirillova, E. N., Budhavant, K., Tiwari, S., Praveen, P. S., Russell, L. M., Beres, N. D., Ramanathan, V., and Gustafsson, Ö.: Source-diagnostic dual-isotope composition and optical properties of water-soluble organic carbon and elemental carbon in the South Asian outflow intercepted over the Indian Ocean, J. Geophys. Res.-Atmos., 119, 11743–11759, https://doi.org/10.1002/2014jd022127, 2014.

Cao, J.-J., Chow, J. C., Tao, J., Lee, S.-C., Watson, J. G., Ho, K.-F., Wang, G.-H., Zhu, C.-S., and Han, Y.-M.: Stable carbon isotopes in aerosols from Chinese cities: Influence of fossil fuels, Atmos. Environ., 45, 1359–1363, https://doi.org/10.1016/j.atmosenv.2010.10.056, 2011.

Carlton, A. G., Turpin, B. J., Altieri, K. E., Seitzinger, S., Reff, A., Lim, H.-J., and Ervens, B.: Atmospheric oxalic acid and SOA production from glyoxal: Results of aqueous photooxidation experiments, Atmos. Environ., 41, 7588–7602, https://doi.org/10.1016/j.atmosenv.2007.05.035, 2007.

Carlton, A. G., Wiedinmyer, C., and Kroll, J. H.: A review of Secondary Organic Aerosol (SOA) formation from isoprene, Atmos.

Chem. Phys., 9, 4987–5005, https://doi.org/10.5194/acp-9-4987-2009, 2009.

Chang, X., Zhao, B., Zheng, H., Wang, S., Cai, S., Guo, F., Gui, P., Huang, G., Wu, D., Han, L., Xing, J., Man, H., Hu, R., Liang, C., Xu, Q., Qiu, X., Ding, D., Liu, K., Han, R., Robinson, A. L., and Donahue, N. M.: Full-volatility emission framework corrects missing and underestimated secondary organic aerosol sources, One Earth, 5, 403–412, https://doi.org/10.1016/j.oneear.2022.03.015, 2022.

Chen, Y., Guo, H., Nah, T., Tanner, D. J., Sullivan, A. P., Takeuchi, M., Gao, Z., Vasilakos, P., Russell, A. G., Baumann, K., Huey, L. G., Weber, R. J., and Ng, N. L.: Low-Molecular-Weight Carboxylic Acids in the Southeastern U.S.: Formation, Partitioning, and Implications for Organic Aerosol Aging, Environ. Sci. Technol., 55, 6688–6699, https://doi.org/10.1021/acs.est.1c01413, 2021.

Dasari, S., Andersson, A., Bikkina, S., Holmstrand, H., Budhavant, K., Satheesh, S., Asmi, E., Kesti, J., Backman, J., Salam, A., Bisht, D. S., Tiwari, S., Hameed, Z., and Gustafsson, Ö.: Photochemical degradation affects the light absorption of water-soluble brown carbon in the South Asian outflow, Sci. Adv., 5, eaau8066, https://doi.org/10.1126/sciadv.aau8066, 2019.

Elmquist, M., Cornelissen, G., Kukulska, Z., and Gustafsson, O.: Distinct oxidative stabilities of char versus soot black carbon: Implications for quantification and environmental recalcitrance, Global Biogeochem. Cy., 20, GB2009, https://doi.org/10.1029/2005gb002629, 2006.

Ervens, B., Turpin, B. J., and Weber, R. J.: Secondary organic aerosol formation in cloud droplets and aqueous particles (aqSOA): a review of laboratory, field and model studies, Atmos. Chem. Phys., 11, 11069–11102, https://doi.org/10.5194/acp-11-11069-2011, 2011.

Fang, W., Du, K., Andersson, A., Xing, Z., Cho, C., Kim, S.-W., Deng, J., and Gustafsson, Ö.: Dual-Isotope Constraints on Seasonally Resolved Source Fingerprinting of Black Carbon Aerosols in Sites of the Four Emission Hot Spot Regions of China, J. Geophys. Res.-Atmos., 123, 11735–11747, https://doi.org/10.1029/2018jd028607, 2018.

Fisseha, R., Spahn, H., Wegener, R., Hohaus, T., Brasse, G., Wissel, H., Tillmann, R., Wahner, A., Koppmann, R., and Kiendler-Scharr, A.: Stable carbon isotope composition of secondary organic aerosol from β-pinene oxidation, J. Geophys. Res.-Atmos., 114, D02304, https://doi.org/10.1029/2008jd011326, 2009.

Fu, T.-M., Jacob, D. J., Wittrock, F., Burrows, J. P., Vrekoussis, M., and Henze, D. K.: Global budgets of atmospheric glyoxal and methylglyoxal, and implications for formation of secondary organic aerosols, J. Geophys. Res.-Atmos., 113, D15303, https://doi.org/10.1029/2007jd009505, 2008.

Gkatzelis, G. I., Papanastasiou, D. K., Karydis, V. A., Hohaus, T., Liu, Y., Schmitt, S. H., Schlag, P., Fuchs, H., Novelli, A., Chen, Q., Cheng, X., Broch, S., Dong, H., Holland, F., Li, X., Liu, Y., Ma, X., Reimer, D., Rohrer, F., Shao, M., Tan, Z., Taraborrelli, D., Tillmann, R., Wang, H., Wang, Y., Wu, Y., Wu, Z., Zeng, L., Zheng, J., Hu, M., Lu, K., Hofzumahaus, A., Zhang, Y., Wahner, A., and Kiendler-Scharr, A.: Uptake of water-soluble gas-phase oxidation products drives organic particulate pollution in Beijing, Geophys. Res. Lett., 48, e2020GL091351, https://doi.org/10.1029/2020GL091351, 2021.

Gustafsson, Ö., Kruså, M., Zencak, Z., Sheesley, R. J., Granat, L., Engström, E., Praveen, P. S., Rao, P. S. P., Leck, C., and Rodhe, H.: Brown Clouds over South Asia: Biomass or Fossil Fuel Combustion, Science, 323, 495–498, https://doi.org/10.1126/science.1164857, 2009.

Hallquist, M., Wenger, J. C., Baltensperger, U., Rudich, Y., Simpson, D., Claeys, M., Dommen, J., Donahue, N. M., George, C., Goldstein, A. H., Hamilton, J. F., Herrmann, H., Hoffmann, T., Iinuma, Y., Jang, M., Jenkin, M. E., Jimenez, J. L., Kiendler-Scharr, A., Maenhaut, W., McFiggans, G., Mentel, Th. F., Monod, A., Prévôt, A. S. H., Seinfeld, J. H., Surratt, J. D., Szmigielski, R., and Wildt, J.: The formation, properties and impact of secondary organic aerosol: current and emerging issues, Atmos. Chem. Phys., 9, 5155–5236, https://doi.org/10.5194/acp-9-5155-2009, 2009.

Ho, K. F., Lee, S. C., Cao, J. J., Kawamura, K., Watanabe, T., Cheng, Y., and Chow, J. C.: Dicarboxylic acids, ketocarboxylic acids and dicarbonyls in the urban roadside area of Hong Kong, Atmos. Environ., 40, 3030–3040, https://doi.org/10.1016/j.atmosenv.2005.11.069, 2006.

Ho, K. F., Cao, J. J., Lee, S. C., Kawamura, K., Zhang, R. J., Chow, J. C., and Watson, J. G.: Dicarboxylic acids, ketocarboxylic acids, and dicarbonyls in the urban atmosphere of China, J. Geophys. Res.-Atmos., 112, D22S27, https://doi.org/10.1029/2006JD008011, 2007.

Huang, L., Brook, J. R., Zhang, W., Li, S. M., Graham, L., Ernst, D., Chivulescu, A., and Lu, G.: Stable isotope measurements of carbon fractions (OC/EC) in airborne particulate: A new dimension for source characterization and apportionment, Atmos. Environ., 40, 2690–2705, https://doi.org/10.1016/j.atmosenv.2005.11.062, 2006.

Huang, R.-J., Zhang, Y., Bozzetti, C., Ho, K.-F., Cao, J.-J., Han, Y., Daellenbach, K. R., Slowik, J. G., Platt, S. M., Canonaco, F., Zotter, P., Wolf, R., Pieber, S. M., Bruns, E. A., Crippa, M., Ciarelli, G., Piazzalunga, A., Schwikowski, M., Abbaszade, G., Schnelle-Kreis, J., Zimmermann, R., An, Z., Szidat, S., Baltensperger, U., El Haddad, I., and Prevot, A. S. H.: High secondary aerosol contribution to particulate pollution during haze events in China, Nature, 514, 218–222, 10.1038/nature13774, 2014.

Huang, X.-F. and Yu, J. Z.: Is vehicle exhaust a significant primary source of oxalic acid in ambient aerosols?, Geophys. Res. Lett., 34, L02808, https://doi.org/10.1029/2006gl028457, 2007.

Irei, S., Huang, L., Collin, F., Zhang, W., Hastie, D., and Rudolph, J.: Flow reactor studies of the stable carbon isotope composition of secondary particulate organic matter generated by OH-radical-induced reactions of toluene, Atmos. Environ., 40, 5858–5867, https://doi.org/10.1016/j.atmosenv.2006.05.001, 2006.

Kawamura, K. and Bikkina, S.: A review of dicarboxylic acids and related compounds in atmospheric aerosols: Molecular distributions, sources and transformation, Atmos. Res., 170, 140–160, https://doi.org/10.1016/j.atmosres.2015.11.018, 2016.

Kawashima, H. and Haneishi, Y.: Effects of combustion emissions from the Eurasian continent in winter on seasonal δ^{13}C of elemental carbon in aerosols in Japan, Atmos. Environ., 46, 568–579, https://doi.org/10.1016/j.atmosenv.2011.05.015, 2012.

Kirillova, E. N., Sheesley, R. J., Andersson, A., and Gustafsson, Ö.: Natural abundance ^{13}C and ^{14}C analysis of water-soluble organic carbon in atmospheric aerosols, Anal. Chem., 82, 7973, https://doi.org/10.1021/ac1014436, 2010.

Kirillova, E. N., Andersson, A., Sheesley, R. J., Kruså, M., Praveen, P. S., Budhavant, K., Safai, P. D., Rao, P. S. P., and Gustafsson, Ö.: ^{13}C- and ^{14}C-based study of sources and atmospheric processing of water-soluble organic carbon (WSOC) in South Asian aerosols, J. Geophys. Res.-Atmos., 118, 614–626, https://doi.org/10.1002/jgrd.50130, 2013.

Kirillova, E. N., Andersson, A., Han, J., Lee, M., and Gustafsson, Ö.: Sources and light absorption of water-soluble organic carbon aerosols in the outflow from northern China, Atmos. Chem. Phys., 14, 1413–1422, https://doi.org/10.5194/acp-14-1413-2014, 2014a.

Kirillova, E. N., Andersson, A., Tiwari, S., Srivastava, A. K., Bisht, D. S., and Gustafsson, O.: Water-soluble organic carbon aerosols during a full New Delhi winter: Isotope-based source apportionment and optical properties, J. Geophys. Res.-Atmos., 119, 3476–3485, https://doi.org/10.1002/2013jd020041, 2014b.

Lim, Y. B., Tan, Y., Perri, M. J., Seitzinger, S. P., and Turpin, B. J.: Aqueous chemistry and its role in secondary organic aerosol (SOA) formation, Atmos. Chem. Phys., 10, 10521–10539, https://doi.org/10.5194/acp-10-10521-2010, 2010.

Lim, Y. B., Tan, Y., and Turpin, B. J.: Chemical insights, explicit chemistry, and yields of secondary organic aerosol from OH radical oxidation of methylglyoxal and glyoxal in the aqueous phase, Atmos. Chem. Phys., 13, 8651–8667, https://doi.org/10.5194/acp-13-8651-2013, 2013.

Link, M. F., Brophy, P., Fulgham, S. R., Murschell, T., and Farmer, D. K.: Isoprene versus Monoterpenes as Gas-Phase Organic Acid Precursors in the Atmosphere, ACS Earth Space Chem., 5, 1600–1612, https://doi.org/10.1021/acsearthspacechem.1c00093, 2021.

Liu, D., Li, J., Cheng, Z., Zhong, G., Zhu, S., Ding, P., Shen, C., Tian, C., Chen, Y., Zhi, G., and Zhang, G.: Sources of non-fossil-fuel emissions in carbonaceous aerosols during early winter in Chinese cities, Atmos. Chem. Phys., 17, 11491–11502, https://doi.org/10.5194/acp-17-11491-2017, 2017.

Liu, D., Vonwiller, M., Li, J., Liu, J., Szidat, S., Zhang, Y., Tian, C., Chen, Y., Cheng, Z., Zhong, G., Fu, P., and Zhang, G.: Fossil and Non-fossil Fuel Sources of Organic and Elemental Carbonaceous Aerosol in Beijing, Shanghai, and Guangzhou: Seasonal Carbon Source Variation, Aerosol Air Qual. Res., 20, 2495–2506, https://doi.org/10.4209/aaqr.2019.12.0642, 2020.

Liu, J., Li, J., Zhang, Y., Liu, D., Ding, P., Shen, C., Shen, K., He, Q., Ding, X., Wang, X., Chen, D., Szidat, S., and Zhang, G.: Source apportionment using radiocarbon and organic tracers for $PM_{2.5}$ carbonaceous aerosols in Guangzhou, South China: contrasting local- and regional-scale haze events, Environ. Sci. Technol., 48, 12002–12011, https://doi.org/10.1021/es503102w, 2014.

Liu, J., Li, J., Liu, D., Ding, P., Shen, C., Mo, Y., Wang, X., Luo, C., Cheng, Z., Szidat, S., Zhang, Y., Chen, Y., and Zhang, G.: Source apportionment and dynamic changes of carbonaceous aerosols during the haze bloom-decay process in China based on radiocarbon and organic molecular tracers, Atmos. Chem. Phys., 16, 2985–2996, https://doi.org/10.5194/acp-16-2985-2016, 2016a.

Liu, J., Li, J., Vonwiller, M., Liu, D., Cheng, H., Shen, K., Salazar, G., Agrios, K., Zhang, Y., He, Q., Ding, X., Zhong, G., Wang, X., Szidat, S., and Zhang, G.: The importance of non-fossil sources in carbonaceous aerosols in a megacity of central China during the 2013 winter haze episode: A source apportionment constrained by radiocarbon and organic tracers, Atmos. Environ., 144, 60–68, https://doi.org/10.1016/j.atmosenv.2016.08.068, 2016b.

Lv, S., Wang, F., Wu, C., Chen, Y., Liu, S., Zhang, S., Li, D., Du, W., Zhang, F., Wang, H., Huang, C., Fu, Q., Duan, Y., and Wang, G.: Gas-to-Aerosol Phase Partitioning of Atmospheric Water-Soluble Organic Compounds at a Rural Site in China: An Enhancing Effect of NH_3 on SOA Formation, Environ. Sci. Technol., 56, 3915–3924, https://doi.org/10.1021/acs.est.1c06855, 2022.

Martinelli, L. A., Camargo, P. B., Lara, L., Victoria, R. L., and Artaxo, P.: Stable carbon and nitrogen isotopic composition of bulk aerosol particles in a C_4 plant landscape of southeast Brazil, Atmos. Environ., 36, 2427–2432, https://doi.org/10.1016/s1352-2310(01)00454-x, 2002.

Meng, J., Wang, G., Hou, Z., Liu, X., Wei, B., Wu, C., Cao, C., Wang, J., Li, J., Cao, J., Zhang, E., Dong, J., Liu, J., Ge, S., and Xie, Y.: Molecular distribution and stable carbon isotopic compositions of dicarboxylic acids and related SOA from biogenic sources in the summertime atmosphere of Mt. Tai in the North China Plain, Atmos. Chem. Phys., 18, 15069–15086, https://doi.org/10.5194/acp-18-15069-2018, 2018.

Mo, Y., Li, J., Cheng, Z., Zhong, G., Zhu, S., Tian, C., Chen, Y., and Zhang, G.: Dual carbon isotope-based source apportionment and light absorption properties of water-soluble organic carbon in $PM_{2.5}$ over China, J. Geophys. Res.-Atmos., 126, e2020JD033920, https://doi.org/10.1029/2020JD033920, 2021.

Myriokefalitakis, S., Tsigaridis, K., Mihalopoulos, N., Sciare, J., Nenes, A., Kawamura, K., Segers, A., and Kanakidou, M.: In-cloud oxalate formation in the global troposphere: a 3-D modeling study, Atmos. Chem. Phys., 11, 5761–5782, https://doi.org/10.5194/acp-11-5761-2011, 2011.

Pavuluri, C. M. and Kawamura, K.: Evidence for 13-carbon enrichment in oxalic acid via iron catalyzed photolysis in aqueous phase, Geophys. Res. Lett., 39, L03802, https://doi.org/10.1029/2011gl050398, 2012.

Pavuluri, C. M., Kawamura, K., and Swaminathan, T.: Water-soluble organic carbon, dicarboxylic acids, ketoacids, and α-dicarbonyls in the tropical Indian aerosols, J. Geophys. Res.-Atmos., 115, D11302, https://doi.org/10.1029/2009jd012661, 2010.

Pavuluri, C. M., Kawamura, K., Swaminathan, T., and Tachibana, E.: Stable carbon isotopic compositions of total carbon, dicarboxylic acids and glyoxylic acid in the tropical Indian aerosols: Implications for sources and photochemical processing of organic aerosols, J. Geophys. Res.-Atmos., 116, D18307, https://doi.org/10.1029/2011jd015617, 2011.

Qi, W., Wang, G., Dai, W., Liu, S., Zhang, T., Wu, C., Li, J., Shen, M., Guo, X., Meng, J., and Li, J.: Molecular characteristics and stable carbon isotope compositions of dicarboxylic acids and related compounds in wintertime aerosols of Northwest China, Sci. Rep., 12, 11266, https://doi.org/10.1038/s41598-022-15222-6, 2022.

Qiu, X., Duan, L., Chai, F., Wang, S., Yu, Q., and Wang, S.: Deriving High-Resolution Emission Inventory of Open Biomass Burning in China based on Satellite Observations, Environ. Sci. Technol., 50, 11779–11786, https://doi.org/10.1021/acs.est.6b02705, 2016.

Shen, M., Ho, K. F., Dai, W., Liu, S., Zhang, T., Wang, Q., Meng, J., Chow, J. C., Watson, J. G., Cao, J., and Li, J.: Distribution and stable carbon isotopic composition of dicarboxylic acids, ketocarboxylic acids and α-dicarbonyls in fresh and aged biomass burning aerosols, Atmos. Chem. Phys., 22, 7489–7504, https://doi.org/10.5194/acp-22-7489-2022, 2022.

Smith, B. N. and Epstein, S.: Two categories of $^{13}C/^{12}C$ ratios for higher plants, Plant Physiol., 47, 380–384, https://doi.org/10.1104/pp.47.3.380, 1971.

Szidat, S., Jenk, T. M., Gaggeler, H. W., Synal, H. A., Fisseha, R., Baltensperger, U., Kalberer, M., Samburova, V., Wacker, L., Saurer, M., Schwikowski, M., and Hajdas, I.: Source apportionment of aerosols by C-14 measurements in different carbonaceous particle fractions, Radiocarbon, 46, 475–484, https://doi.org/10.1017/s0033822200039783, 2004.

Szidat, S., Jenk, T. M., Synal, H. A., Kalberer, M., Wacker, L., Hajdas, I., Kasper-Giebl, A., and Baltensperger, U.: Contributions of fossil fuel, biomass-burning, and biogenic emissions to carbonaceous aerosols in Zurich as traced by C-14, J. Geophys. Res.-Atmos., 111, D07206, https://doi.org/10.1029/2005jd006590, 2006.

van Pinxteren, D., Neusüß, C., and Herrmann, H.: On the abundance and source contributions of dicarboxylic acids in size-resolved aerosol particles at continental sites in central Europe, Atmos. Chem. Phys., 14, 3913–3928, https://doi.org/10.5194/acp-14-3913-2014, 2014.

Wang, J., Wang, G., Wu, C., Li, J., Cao, C., Li, J., Xie, Y., Ge, S., Chen, J., Zeng, L., Zhu, T., Zhang, R., and Kawamura, K.: Enhanced aqueous-phase formation of secondary organic aerosols due to the regional biomass burning over North China Plain, Environ. Pollut., 256, 113401, https://doi.org/10.1016/j.envpol.2019.113401, 2020.

Wang, J., Ye, J., Zhang, Q., Zhao, J., Wu, Y., Li, J., Liu, D., Li, W., Zhang, Y., Wu, C., Xie, C., Qin, Y., Lei, Y., Huang, X., Guo, J., Liu, P., Fu, P., Li, Y., Lee, H. C., Choi, H., Zhang, J., Liao, H., Chen, M., Sun, Y., Ge, X., Martin, S. T., and Jacob, D. J.: Aqueous production of secondary organic aerosol from fossil-fuel emissions in winter Beijing haze, P. Natl. Acad. Sci. USA, 118, e2022179118, https://doi.org/10.1073/pnas.2022179118, 2021.

Warneck, P.: In-cloud chemistry opens pathway to the formation of oxalic acid in the marine atmosphere, Atmos. Environ., 37, 2423–2427, https://doi.org/10.1016/S1352-2310(03)00136-5, 2003.

Widory, D., Roy, S., Le Moullec, Y., Goupil, G., Cocherie, A., and Guerrot, C.: The origin of atmospheric particles in Paris: a view through carbon and lead isotopes, Atmos. Environ., 38, 953–961, https://doi.org/10.1016/j.atmosenv.2003.11.001, 2004.

Wu, Z., Wang, Y., Tan, T., Zhu, Y., Li, M., Shang, D., Wang, H., Lu, K., Guo, S., Zeng, L., and Zhang, Y.: Aerosol liquid water driven by anthropogenic inorganic salts: implying its key role in haze formation over the North China Plain, Environ. Sci. Tech. Let., 5, 160–166, https://doi.org/10.1021/acs.estlett.8b00021, 2018.

Xing, J., Lu, X., Wang, S., Wang, T., Ding, D., Yu, S., Shindell, D., Ou, Y., Morawska, L., Li, S., Ren, L., Zhang, Y., Loughlin, D., Zheng, H., Zhao, B., Liu, S., Smith, K. R., and Hao, J.: The quest for improved air quality may push China to continue its CO_2 reduction beyond the Paris Commitment, P. Natl. Acad. Sci. USA, 117, 29535–29542, https://doi.org/10.1073/pnas.2013297117, 2020.

Xu, B., Cheng, Z., Gustafsson, Ö., Kawamura, K., Jin, B., Zhu, S., Tang, T., Zhang, B., Li, J., and Zhang, G.: Compound-specific radiocarbon analysis of low molecular weight dicarboxylic acids in ambient aerosols using preparative gas chromatography: method development, Environ. Sci. Technol. Lett., 8, 135–141, https://doi.org/10.1021/acs.estlett.0c00887, 2021.

Xu, B., Zhang, G., Gustafsson, Ö., Kawamura, K., Li, J., Andersson, A., Bikkina, S., Kunwar, B., Pokhrel, A., Zhong, G., Zhao, S., Li, J., Huang, C., Cheng, Z., Zhu, S., Peng, P., and Sheng, G.: Large contribution of fossil-derived components to aqueous secondary organic aerosols in China, Nat. Commun., 13, 5115, https://doi.org/10.1038/s41467-022-32863-3, 2022.

Yu, Q., Chen, J., Cheng, S., Qin, W., Zhang, Y., Sun, Y., and Ahmad, M.: Seasonal variation of dicarboxylic acids in $PM_{2.5}$ in Beijing: Implications for the formation and aging processes of secondary organic aerosols, Sci. Total Environ., 763, 142964, https://doi.org/10.1016/j.scitotenv.2020.142964, 2021.

Zhang, G., Liu, J., Li, J., Li, P., Wei, N., and Xu, B.: Radiocarbon isotope technique as a powerful tool in tracking anthropogenic emissions of carbonaceous air pollutants and greenhouse gases: A review, Fundam. Res., 1, 306–316, https://doi.org/10.1016/j.fmre.2021.03.007, 2021.

Zhang, Y., Ren, H., Sun, Y., Cao, F., Chang, Y., Liu, S., Lee, X., Agrios, K., Kawamura, K., Liu, D., Ren, L., Du, W., Wang, Z., Prévôt, A. S. H., Szidat, S., and Fu, P.: High Contribution of Nonfossil Sources to Submicrometer Organic Aerosols in Beijing, China, Environ. Sci. Technol., 51, 7842–7852, https://doi.org/10.1021/acs.est.7b01517, 2017.

Zhang, Y.-L., Schnelle-Kreis, J., Abbaszade, G., Zimmermann, R., Zotter, P., Shen, R.-R., Schaefer, K., Shao, L., Prevot, A. S. H., and Szidat, S.: Source Apportionment of Elemental Carbon in Beijing, China: Insights from Radiocarbon and Organic Marker Measurements, Environ. Sci. Technol., 49, 8408–8415, https://doi.org/10.1021/acs.est.5b01944, 2015.

Zhang, Y.-L., Kawamura, K., Cao, F., and Lee, M.: Stable carbon isotopic compositions of low-molecular-weight dicarboxylic acids, oxocarboxylic acids, α-dicarbonyls, and fatty acids: Implications for atmospheric processing of organic aerosols, J. Geophys. Res.-Atmos., 121, 3707–3717, https://doi.org/10.1002/2015jd024081, 2016.

Zhao, B., Zheng, H., Wang, S., Smith, K. R., Lu, X., Aunan, K., Gu, Y., Wang, Y., Ding, D., Xing, J., Fu, X., Yang, X., Liou, K.-N., and Hao, J.: Change in household fuels dominates the decrease in $PM_{2.5}$ exposure and premature mortality in China in 2005–2015, P. Natl. Acad. Sci. USA, 115, 12401–12406, https://doi.org/10.1073/pnas.1812955115, 2018.

Zhao, S., Tian, L., Zou, Z., Liu, X., Zhong, G., Mo, Y., Wang, Y., Tian, Y., Li, J., Guo, H., and Zhang, G.: Probing Legacy and Alternative Flame Retardants in the Air of Chinese Cities, Environ. Sci. Technol., 55, 9450–9459, https://doi.org/10.1021/acs.est.0c07367, 2021.

Zhu, S., Ding, P., Wang, N., Shen, C., Jia, G., and Zhang, G.: The compact AMS facility at Guangzhou Institute of Geochemistry, Chinese Academy of Sciences, Nucl. Instrum. Meth. B, 361, 72–75, https://doi.org/10.1016/j.nimb.2015.06.040, 2015.